Iron carbonyl complexes bearing phenazine and acridine ligands: X-ray structures of $Fe(CO)_3(\eta^4\text{-}C_{12}H_8N_2)$, $Fe(CO)_2\{P(OMe)_3\}(\eta^4\text{-}C_{12}H_8N_2)$, $Fe(CO)_2(PPh_3)(\eta^4\text{-}C_{13}H_9N)$, and $Fe(CO)_2(\kappa^1\text{-dppm})(\eta^4\text{-}C_{12}H_8N_2)$

Md. Arshad H. Chowdhury[a], Md. Saifur Rahman [a], Md. Rakibul Islam[a], Subas Rajbangshi[a], Shishir Ghosh[a], Graeme Hogarth[b], Derek A. Tocher[c], Li Yang[d], Michael G. Richmond[d], Shariff E. Kabir [a,*]

[a]*Department of Chemistry, Jahangirnagar University, Savar, Dhaka 1342, Bangladesh*

[b]*Department of Chemistry, King's College London, Britannia House, 7 Trinity Street, London SE1 1DB, UK*

[c]*Department of Chemistry, University College London, 20 Gordon Street, London WC1H OAJ, UK*

[d]*Department of Chemistry, University of North Texas, Denton, TX 76209, USA*

* Corresponding author.
E-mail address: skabir_ju@yahoo.com (S.E. Kabir).
Tel.: +880 27791099; fax: +880 27791052.

Abstract

Reactions of $Fe_3(CO)_{12}$ with the heterocycles phenazine and acridine in refluxing benzene afforded the mononuclear complexes $Fe(CO)_3(\eta^4\text{-}C_{12}H_8N_2)$ (**1a**) and $Fe(CO)_3(\eta^4\text{-}C_{13}H_9N)$ (**1b**), respectively. Treatment of **1a** with $P(OMe)_3$ and PPh_3 in the presence of Me_3NO at room temperature yielded the carbonyl substitution products $Fe(CO)_2\{P(OMe)_3\}(\eta^4\text{-}C_{12}H_8N_2)$ (**2a**) and $Fe(CO)_2(PPh_3)(\eta^4\text{-}C_{12}H_8N_2)$ (**3a**), respectively. Similar reactions of **1b** yielded $Fe(CO)_2\{P(OMe)_3\}(\eta^4\text{-}C_{13}H_9N)$ (**2b**) and $Fe(CO)_2(PPh_3)(\eta^4\text{-}C_{13}H_9N)$ (**3b**). Treatment of **1a** with the diphosphines dppm and dppf under similar conditions afforded the mononuclear compounds $Fe(CO)_2(\kappa^1\text{-dppm})(\eta^4\text{-}C_{12}H_8N_2)$ (**4a**) and $Fe(CO)_2(\kappa^1\text{-dppf})(\eta^4\text{-}C_{12}H_8N_2)$ (**4b**). Compounds **1a**, **2a**, **3b**, and **4a** have been structurally characterized by X-ray crystallography. The ancillary phenazine and acridine ligands in these products adopt an η^4-coordination mode by using only the peripheral carbon atoms in one of the carbocyclic rings. Given the rarity of this coordination mode in metal carbonyl complexes, we have performed electronic structure calculations on **1a** and these data are discussed relative to the solid-state structure.

Keywords: Iron carbonyl; Phenazine; Acridine; Phosphines; X-ray structure; DFT calculations

1. Introduction

Phenazine, a bisannulated derivative of pyrazine, is a planar *N*-heterocyclic ligand whose biological and spectral properties have been extensively studied in the fields of chemistry and biology.[1,2,3,4,5,6,7,8] Although similar to the parent heterocycle, pyrazine, with respect to its N-based coordination chemistry, it has different electronic and steric properties, which in turn give rise to ligand coordination modes and unique structural motifs for those compounds that possess an ancillary phenazine. Phenazine possesses idealized D_{2h} symmetry similar to pyrazine, but the presence of the fused benzene rings at the pyrazine junctions imparts additional steric bulk to phenazine related to the parent heterocycle and the monoannulated derivative quinoxaline. As an ancillary ligand, phenazine is known to exhibit terminal[9] and bridging[10] coordination modes, as well as functioning as an electron donor in intermolecular arrays by directing the formation of columnar stacks through π-π interactions.[11] Acridine

contains only one nitrogen atom and its structural properties and reactivity often mimic that of phenazine.

As early as 1970 Fischer and co-workers reported reactions a range of condensed aromatic compounds with $Fe_3(CO)_{12}$ at elevated temperatures, including the reaction with phenazine with lead to the formation of $Fe(CO)_3(\eta^4\text{-}C_{12}H_8N_2)$ (**1a**) in 34% yield.[12] While this complex was characterised spectroscopically, at the time a crystal structure was not obtained and the precise perturbations of the aromatic system upon complexation were not elucidated. More recently Ellis and co-workers reported the synthesis and crystal structure of the anthracene complex $[K(L)(thf)_2][Fe(\eta^4\text{-}C_{14}H_{10})_2]$ (L = 2,2,2-crypt) which shows that the coordinated anthracene ligands are highly distorted away from their planar aromatic forms upon metal coordination.[13] While the reactivity of the triruthenium and triosmium clusters $M_3(CO)_{12-n}(NCMe)_n$ with the nitrogen heterocycles pyridine,[14,15,16,17] pyrazole,[14] pyrimidine,[18,19] pyrazine,[18,20] quinoxaline,[20] and quinoline[18,21,22,23] has been extensively been investigated, few studies have hitherto been published involving the heterocycle phenazine. Cabeza et al.[24] recently reported that the reaction of $Ru_3(CO)_{12}$ with phenazine in refluxing THF led to the formation of tri-, tetra- and hexanuclear clusters $Ru_3(CO)_9(\mu_3\text{-}\{(C_6H_4)(C_6H_3)N_2\}(\mu\text{-}H)$, $Ru_4(CO)_{10}(\mu\text{-}CO)(\mu_4\text{-}\{(C_6H_4)(C_6H_3)N_2H\}$ and $Ru_6(CO)_{12}(\mu\text{-}CO)(\mu_5\text{-}\{(C_6H_4)(C_6H_3)N_2H\}$ (Scheme 1).

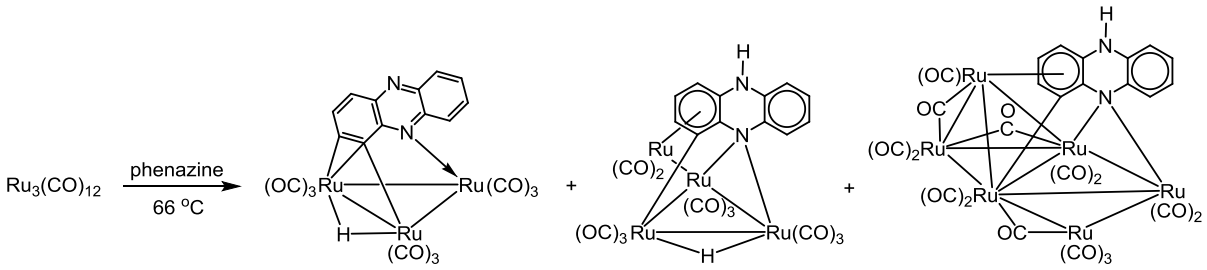

Scheme 1. Reaction of $Ru_3(CO)_{12}$ with phenazine

More recently, we reported the isolation and structural characterization of the face-capped monohydride $Os_3(CO)_9(\mu_3\text{-}\eta^2\text{-}C_{12}H_7N_2)(\mu\text{-}H)$ and electron-precise dihydride $Os_3(CO)_9(\mu_3\text{-}\eta^2\text{-}C_{12}H_6N_2)(\mu\text{-}H)_2$ clusters from the reaction of $Os_3(CO)_{12}$ with phenazine in refluxing xylene (Scheme 2).[25]

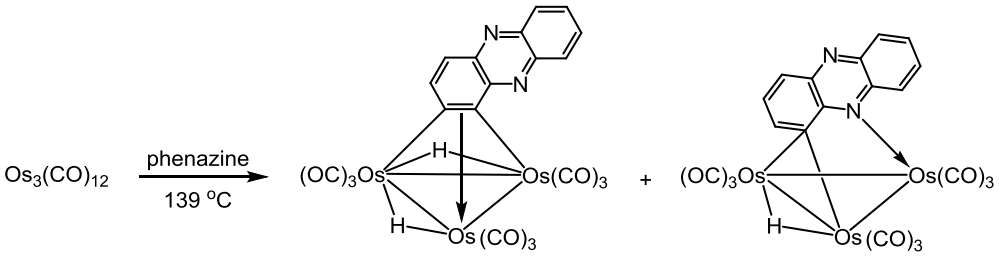

Scheme 1. Reaction of $Os_3(CO)_{12}$ with phenazine

In order to complete the study of phenazine reactivity with the Group 8 trimetallic clusters, we have investigated the reaction of $Fe_3(CO)_{12}$ with phenazine. Herein, we report our results on the mononuclear iron compound $Fe(CO)_3(\eta^4\text{-}C_{12}H_8N_2)$ (**1a**), which was isolated from the thermolysis of $Fe_3(CO)_{12}$ in the presence of phenazine. Also reported is the reactivity of acridine with $Fe_3(CO)_{12}$ under analogous conditions, which furnishes $Fe(CO)_3(\eta^4\text{-}C_{13}H_9N)$ (**1b**). Our data reveal that the two heterocyclic ligands adopt a different coordination mode in the case of iron compared to the products found in the related reactions using ruthenium and osmium carbonyl cluster complexes.

2. Experimental

2.1. General procedures

Unless otherwise noted, all reactions were carried out under a nitrogen atmosphere using standard Schlenk techniques. Reagent-grade solvents were dried using appropriate drying agents and distilled prior to use by standard methods. $Fe_3(CO)_{12}$ was prepared according to the published procedure.[26] Phenazine and acridine were purchased from Sigma-Aldrich and used without further purification. $Me_3NO{\cdot}2H_2O$ was dried by azeotropic distillation using benzene with Dean–Stark distillation equipment. Infrared spectra were recorded on a Shimadzu IR Prestige-21 spectrophotometer, and the ^1H and ^{13}C NMR spectra were recorded on a Varian Unity 500 NMR spectrometer. The spectral assignments for **1a** were ascertained through a combination of 2D NMR experiments, including ^1H COSY, HMQC, and HMBC techniques. All chemical shifts are reported in δ units and are referenced to the residual protons of the deuterated solvents (^1H and ^{13}C) and external 85% H_3PO_4 (^{31}P) as appropriate. Elemental analyses were performed by the Microanalytical Laboratories of the Wazed Miah

Science Research Centre at Jahangirnagar University. Product separations were performed by TLC in air on 0.5 mm silica gel (GF_{254}-type 60, E. Merck, Germany) glass plates.

2.2. Reaction of $Fe_3(CO)_{12}$ with phenazine

A benzene solution (25 mL) containing $Fe_3(CO)_{12}$ (0.20 g, 0.40 mmol) and phenazine (71 mg, 0.39 mmol) was heated to reflux for 3 h. The solvent was removed under reduced pressure and the residue chromatographed by TLC on silica gel. Elution with cyclohexane/CH_2Cl_2 (2:3, v/v) developed four bands. The slowest moving band afforded $Fe(CO)_3(\eta^4\text{-}C_{12}N_2H_8)$ (**1a**) (0.18 g, 47%) as orange crystals after recrystallization from dichloromethane/hexane at 4 ^oC. The first and second bands were too small for complete characterization, while the third band afforded unreacted phenazine. Spectral data for **1a:** IR (νCO, CH_2Cl_2): 2064 vs, 2005 vs, 1997 sh cm^{-1}. ^1H NMR (CD_2Cl_2): δ 3.87 (AA′, diene, J = 5.4, 3.5 Hz, 2H), 6.53 (XX′, diene, J = 5.4, 3.5 Hz, 2H), 7.38 (AA′, aryl, J = 6.5, 3.0 Hz, 2H), 7.51 (BB′, J = 6.5, 3.0 Hz, 2H). ^{13}C NMR (CD_2Cl_2): δ 62. 14 (CH), 88.03 (CH), 127.55 (CH), 128.18 (CH), 139.46 (C), 156.98 (C), 207.25 (Fe-CO). Anal. Calcd. for $C_{15}H_8FeN_2O_3$: C, 56.29; H, 2.52; N, 8.75. Found: C, 56.55; H, 2.72; N, 8.83%. A similar reaction between $Fe_2(CO)_9$ (50 mg, 0.14 mmol) and phenazine (25 mg, 0.14 mmol), followed by similar chromatographic separation, afforded **1a** (18 mg, 20%), while use of $Fe(CO)_5$ (50 mg, 0.26 mmol) as the iron precursor (46 mg, 0.26 mmol) also furnished **1a** (15 mg, 18%).

2.3 Reaction of $Fe_3(CO)_{12}$ with acridine

A benzene solution (25 mL) of $Fe_3(CO)_{12}$ (0.10 g, 0.20 mmol) and acridine (0.11 g, 0.59 mmol) was heated to reflux for 1.5 h and then allowed to cool to room temperature. The solvent was removed under reduced pressure and the residue chromatographed by TLC on silica gel. Elution with cyclohexane/acetone (4:1, v/v) developed four bands. The third band gave $Fe(CO)_3(\eta^4\text{-}C_{13}H_9N)$ (**1b**) (66 mg, 35%) as orange crystals after recrystalliazation from hexane/CH_2Cl_2 at 4 ^oC. The first and the fourth bands corresponded to unreacted $Fe_3(CO)_{12}$ and acridine, respectively. The second band was too small for complete characterization. Spectral data for **1b**: IR (νCO, CH_2Cl_2): 2057 vs, 1995 s, 1983 sh cm^{-1}. ^1H NMR ($CDCl_3$): δ 7.65 (d, 1H, J = 5.5 Hz), 7.41 (d, 2H, J = 5.5 Hz), 7.28 (s, 1H), 7.14 (s, 1H), 6.56 (s, 1H), 6.40

(s, 1H), 3.88 (s, 1H), 3.77 (s, 1H). Anal. Calcd. for $C_{16}H_9FeNO_3$: C, 60.22; H, 2.84; N, 4.39. Found: C, 60.42: H, 3.05; N, 4.58%.

*2.4. Reaction of **1a** with $P(OMe)_3$*

To a dichloromethane solution (20 mL) of **1** (20 mg, 0.06 mmol) and $P(OMe)_3$ (15 μL, 0.12 mmol) was added dropwise a solution of Me_3NO (5 mg, 0.07 mmol) in the same solvent (10 mL) and the solution was stirred at room temperature for 2h. The solution was then filtered through a short silica column (4 cm), followed by solvent removal under reduced pressure. The resulting residue was purified by chromatography over silica gel using cyclohexane/CH_2Cl_2 (1:9, v/v) as the eluent. Of the two developed two bands, the faster moving band corresponded to unconsumed **1a** (trace), while the slower moving bond yielded $Fe(CO)_2\{P(OMe)_3\}(\eta^4\text{-}C_{12}H_8N_2)$ (**2a**) (23 mg, 88%). The analytical sample of **2a** was isolated as red crystals after recrystallization from hexane/CH_2Cl_2 at 4 ^oC. Spectral data for **2a**: IR (νCO, CH_2Cl_2): 2008 vs, 1954 vs cm^{-1}. ^1H NMR ($CDCl_3$): δ 7.47 (m, 2H), 7.31 (m, 2H), 6.23 (m, 2H), 3.62 (m, 2H), 3.58 (d, *J* = 15.0 Hz, 9H). $^{31}P\{^1H\}$NMR ($CDCl_3$): δ 174.6 (s). Anal. Calcd. for $C_{17}H_{17}FeN_2O_5P$: C, 49.07; H, 4.12; N, 6.73. Found: C, 49.22; H, 4.28; N, 6.88%.

*2.5. Reaction of **1b** with $P(OMe)_3$*

A similar reaction between **1b** (20 mg, 0.06 mmol) and $P(OMe)_3$ (15 μL, 0.12 mmol) in the presence of Me_3NO (5 mg, 0.07 mmol) yielded $Fe(CO)_2\{P(OMe)_3\}(\eta^4\text{-}C_{13}H_9N)$ (**2b**) (21 mg, 80%) as red crystals after recrystallization from hexane/CH_2Cl_2 at 4 ^oC. Spectral data for **2b**: IR (νCO, CH_2Cl_2): 1999 (vs), 1943 (vs) cm^{-1}.^1H NMR ($CDCl_3$): δ 7.58 (d, *J* = 8.4 Hz, 1H), 7.32 (t, *J* = 8.0 Hz, 2H), 7.19 (t, *J* = 8.0 Hz, 1H), 6.97 (s, 1H), 6.23 (s, 1H), 6.08 (s, 1H), 3.61 (m, 1H), 3.58 (d, *J* = 11.6 Hz, 9H), 3.45 (d, *J* = 6.0 Hz, 1H). $^{31}P\{^1H\}$NMR ($CDCl_3$): δ 177.1 (s). Anal. Calcd. for $C_{18}H_{18}FeNO_5P$: C, 52.08; H, 4.37; N, 3.37. Found: C, 52.28; H, 4.55; N, 3.48%.

*2.6. Reaction of **1a** with PPh_3*

To a dichloromethane solution (20 ml) of **1a** (40 mg, 0.13 mmol) and triphenylphosphine (33 mg, 0.126 mmol) was added dropwise a CH_2Cl_2 solution containing Me_3NO (10 mg, 0.13

mmol), followed by stirring at room temperature for 2h. Filtration of the crude reaction mixture through a short silica column (4 cm), followed by solvent removal, afforded the crude product. Chromatographic purification using cyclohexane/dicloromethane (2:3, v/v) developed four bands, of which the first band was confirmed as unreacted triphenylphosphine. The second band was too small for complete characterization and the third band was phenazine (trace). The fourth band gave the desired product $[Fe(CO)_2(PPh_3)(\eta^4\text{-}C_{12}H_8N_2)]$ (**3a**) (66 mg, 95%) as red crystals after recrystallization from dichloromethane/hexane at 4 ^oC. Spectral data for **3a**: IR (νCO, CH_2Cl_2): 1997 (vs), 1943 (vs) cm^{-1}. ^1H NMR ($CDCl_3$): δ 7.44 (m, 17H), 7.39 (m, 2H), 5.98 (m, 2H), 3.30 (m, 2H). $^{31}P\{^1H\}$ NMR ($CDCl_3$): δ 67.0 (s). Anal. Calcd. for $C_{32}FeH_{23}N_2O_2P$: C, 69.30; H, 4.18; N, 5.05. Found: C, 69.60: H, 4.40; N, 5.15%.

*2.7. Reaction of **1b** with PPh_3*

A similar reaction between **1b** (26 mg, 0.08 mmol) and triphenylphosphine (21 mg, 0.08 mmol) in the presence of Me_3NO (6 mg, 0.08 mmol) was conducted and $Fe(CO)_2(PPh_3)(\eta^4\text{-}C_{13}H_9N)$ (**3b**) (40 mg, 88%) was isolated as red crystals after recrystalization from dichloromethane/hexane at 4 ^oC. Spectral data for **3b:** IR (νCO, CH_2Cl_2): 1988 (vs), 1933 (vs) cm^{-1}. ^1H NMR ($CDCl_3$): δ 7.60 (d, J = 8.0 Hz, 1H), 7.43 (m, 15H), 7.33 (t, J = 8.0 Hz, 2H), 7.19 (t, J = 8.0 Hz, 1H), 6.84 (s, 1H), 6.06 (s, 1H), 5.90 (s, 1H), 3.38 (s, 1H), 2.98 (s, 1H). $^{31}P\{^1H\}$ NMR ($CDCl_3$): δ 66.6 (s). Anal. Calcd. for $C_{33}H_{24}FeNO_2P$: C, 71.62; H, 4.37; N, 2.53. Found: C, 71.79: H, 4.46; N, 5.56%.

*2.9. Reaction of **1a** with dppm*

To a dichloromethane solution of **1a** (20 mg, 0.06 mmol) and dppm (24 mg, 0.06 mmol) was added dropwise a solution of Me_3NO (5 mg, 0.07 mmol) in the same solvent (10 mL) and stirring continued for 2 h at room temperature. The solution was filtered through a short silica column (4 cm), after which time the solvent was removed under reduced pressure and the residue chromatographed by TLC on silica gel. Elution with cyclohexane/ CH_2Cl_2 (1:9, v/v) developed two bands. The faster moving band afforded $Fe(CO)_2)(\kappa^1\text{-dppm})(\eta^4\text{-}C_{12}H_8N_2)$ (**4a**) (18 mg, 40%) and slower moving band was isolated in an insufficient amount for spectroscopic characterization. Spectral data for **4a:** IR (νCO, CH_2Cl_2): 1996 (vs), 1942 (vs) cm^{-1}. ^1H NMR($CDCl_3$): δ 7.36 (m, 6H), 7.28 (m, 18H), 6.04 (m, 4H), 3.23 (m, 1H), 3.04 (m,

1H). $^{31}P\{^{1}H\}$ NMR ($CDCl_3$): δ 57.5 (d, *J* = 76.0 Hz, 1P), -24.2 (d, *J* = 76.0 Hz, 1P). Anal. Calcd. for $C_{39}H_{30}FeN_2O_2P_2$: C, 69.25; H, 4.47; N, 4.14. Found: C, 69.42; H, 4.62; N, 4.32%.

*2.8. Reaction of **1a** with dppf*

To a dichloromethane solution (20 mL) of **1a** (20 mg, 0.06 mmol) and dppf (35 mg, 0.06 mmol) was added dropwise a CH_2Cl_2 solution (10 mL) of Me_3NO (5 mg, 0.07 mmol) over a period of 30 min and stirred for an additional 5 h at room temperature. The reaction mixture was then filtered through a short silica column (4 cm). The solvent was removed under reduced pressure and the residue chromatographed by TLC on silica gel. Elution with cyclohexane/dichloromethane (3:7, v/v) developed four bands. The first and second bands were unreacted dppf and phenazine, respectively. The third gave $Fe(CO)_2(\kappa^1\text{-dppf})(\eta^4\text{-}C_{12}H_8N_2)$ (**5a**) (21 mg, 40%) while the fourth band afforded a trace amount of material insufficient for characterization. Spectral data for **5a:** IR (*ν*CO, CH_2Cl_2): 1994(vs), 1941(vs) cm^{-1}. ^{1}H NMR ($CDCl_3$): δ 7.43 (m, 20H), 7.23 (m, 4H), 5.91 (m, 2H), 4.45 (m, 2H), 4.22 (m, 2H), 3.86 (m, 2H), 3.70 (m, 2H), 3.06 (m, 2H). $^{31}P\{^{1}H\}$ NMR ($CDCl_3$): δ 61.0 (s, 1P) -18.1 (s, 1P). Anal. Calcd. for $C_{48}H_{36}Fe_2N_2O_2P_2$: C, 68.11; H, 4.29; N, 3.31. Found: C, 68.31; H, 4.42; N, 3.46%.

2.9. X-ray crystallography

Single crystals were grown by diffusion of hexane into a CH_2Cl_2 solution of **1a**, **2a**, **3b** and **4a**. Single crystals of **1a** and **4a** were mounted on glass fibres and all geometric and intensity data were taken from these samples using a Bruker SMART APEX CCD diffractometer using graphite-monochromated Mo-K*α* radiation (λ = 0.71073 Å) at 150 ± 2 K. Data collection, indexing and initial cell refinements were all done using SMART software.[27] Data reduction were carried out with SAINT PLUS[28] and absorption corrections applied using the programme SADABS.[29] Single crystals of **2a** and **3b** were mounted on a SuperNova, Dual, Cu at zero, Atlas diffractometer and the crystal were kept at 150 K during data collection. Using Olex2,[30] the structures were solved with the structure solution program using ShelXS[31] and refined with the olex2.refine refinement package[32] using Gauss-Newton minimization.

2.10. Computational details and modeling

The DFT calculations on $Fe(CO)_3(\eta^4\text{-}C_{12}H_8N_2)$ (species **A**) were carried out with the Gaussian 09 package of programs,[33] using the B3LYP hybrid functional. This functional is comprised of Becke's three-parameter hybrid exchange functional (B3)[34] and the correlation functional of Lee, Yang, and Parr (LYP).[35] The iron atom was described with the Stuttgart-Dresden effective core potential and SDD basis set,[36] and the 6-31G(d') basis set[37] was employed for all remaining atoms.

The reported geometry for **A** was fully optimized and the analytical second derivatives were evaluated, confirming that the geometry was an energy minimum (no negative eigenvalues). Unscaled vibrational frequencies were used to make zero-point and thermal corrections to the electronic energies. The computed harmonic frequencies for the carbonyl stretching bands have been scaled using a scaling factor of 0.965. The natural charges and Wiberg indices were computed using Weinhold's natural bond orbital (NBO) program.[38,39] The geometry-optimized structures have been drawn with the *JIMP*2 molecular visualization and manipulation program.[40]

3. Results and discussion

3.1. Reactions of $Fe_3(CO)_{12}$ with phenazine and acridine

Treatment of $Fe_3(CO)_{12}$ with phenazine and acridine in refluxing benzene afforded the mononuclear complexes $Fe(CO)_3(\eta^4\text{-}C_{12}N_2H_8)$ (**1a**) (47% yield) and $Fe(CO)_3(\eta^4\text{-}C_{13}H_9N)$ (**1b**) (35% yield), respectively, which were isolated as orange crystals after chromatographic workup. Both **1a**[12] and **1b** have been characterized by a combination of elemental analysis, IR, and ^{1}H NMR spectroscopy; the solid-structure of **1a** was also determined by single crystal X-ray diffraction analysis.

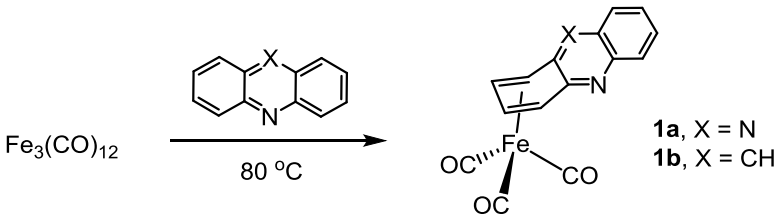

Scheme 3. Reactions of $Fe_3(CO)_{12}$ with phenazine and acridine

The ORTEP drawing of the molecular structure of **1a** is depicted in Fig. 1 (top) and selected bond distances and angles are reported in the figure caption. The molecule contains one iron atom whose coordination sphere consists of three carbonyl ligands and an η^4-$C_{12}H_8N_2$ ligand. The η^4 coordination of the phenazine in **1a** represents a rare bonding mode for this ligand[13]. While η^4-phenazine ligands have been structurally demonstrated by Parkin et al.[41] in a series of molybdenum compounds and by Yang et al.[42] for one nickel diamine complex, no entries of mononuclear iron compounds exist in the Cambridge Structural Database (CSD version 5.36, November 2014). To our knowledge, the iron compounds reported here represent the first such crystallographically characterized examples that the reveal the η^4 coordination of phenazine and acridine ligands. Complex **1a** contains 18e and is electronically saturated, with the CO groups and diene moiety contributing a total of 6e and 4e, respectively to the total electron count. The orientation of the ancillary CO groups relative to the coordinated phenazine is not unlike that found in structurally characterized iron and ruthenium $M(CO)_3(\eta^4$-diene) compounds.[43] The theoretical basis for the preferred disposition of the $Fe,Ru(CO)_3$ rotor relative the polyene framework has been previously addressed.[44] The mean Fe–C bond distance of 2.056 Å for the inner carbon atoms associated with the diene moiety [Fe(1)–C(5) and Fe(1)–C(6)] is 0.10 Å shorter than the mean Fe–C distance for the outer Fe–C(diene) vectors [Fe(1)–C(4) and Fe(1)–C(7)]. Another important aspect of the structure is, as expected, the carbon-carbon bond distances of the coordinated benzo ring [C(4)–C(5) 1.428(3), C(4)–C(9) 1.470(2), C(5)–C(6) 1.399(3), C(6)–C(7) 1.430(3), C(7)–C(8) 1.466(2), C(8)–C(9) 1.437(2) Å] are longer than those of the uncoordinated benzo ring [C(10)–C(11) 1.410(3), C(11)–C(12) 1.411(2), C(12)–C(13) 1.373(3), C(13)–C(14) 1.401(3), C(14)–C(15) 1.375(3), C(10)–C(15) 1.408(3) Å]. The C–N bond distances involving coordinated benzo group [N(1)–C(8) 1.309(2), N(2)–C(9) 1.307(2) Å] are shorter than those of the uncoordinated benzo ring [N(1)–C(11) 1.382(2), N(2)–C(10) 1.392(2) Å]. The DFT optimized structure of **A** is depicted below that of **1a** in Figure 1, and an excellent correspondence exists between the two structures. The Wiberg bond indices (WBI) computed for the heterocyclic scaffold (shown below) parallel the experimentally determined bond lengths and underscore the bond length alterations depicted by the resonance contributor of **1a** in Scheme 3.

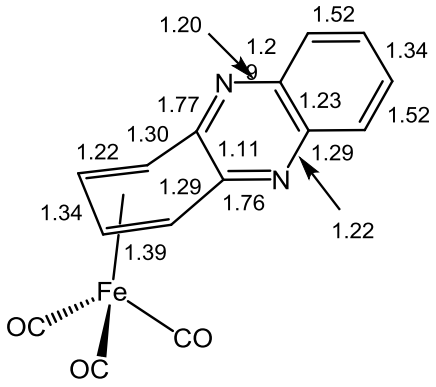

The solution spectroscopic data of **1a** are in complete agreement with the solid-state structure and the earlier work of Fischer.[12] The IR spectrum of **1a** recorded in CH_2Cl_2 reveals three terminal ν(CO) bands at 2065, 2005, and 1997 cm^{-1}, of which the highest energy band corresponds to the symmetric stretching mode for the three vibrationally coupled carbonyl groups. The remaining two ν(CO) bands represent different combinations of antisymmetric stretches involving the carbonyl groups. The nature of these assignments was ascertained by normal mode analysis of the frequency data from the DFT-optimized structure. The ^{1}H NMR spectrum of **1a** (recorded in CD_2Cl_2) shows two different sets of symmetrical spin systems for the eight hydrogens. The diene moiety appears as an AA'XX' system with multiplets centered at δ 3.87 and 6.53, while the remaining four hydrogens on the iron-free aryl ring appear as an AA'BB' spin system. The specific assignments in these spin systems were verified by ^{1}H COSY measurements and the coupling constants were established by spectral simulation using the available program gNMR. The ^{13}C NMR spectrum reveals eight ^{13}C resonances, of which the seven that appear from δ 62.14 to 156.98 belong to the phenazine ligand that possesses idealized C_s symmetry. Rapid tripodal rotation of three CO groups leads to a time-averaged resonance at δ 207.25.[45] The ^{13}C spectral assignments were determined by a combination of HMQC and HMBC experiments, and the below picture shows the specific ^{1}H (black) and ^{13}C (red) NMR assignments for **1a**. The IR and ^{1}H spectral data recorded for **1b** were similar in nature and are summarized in the experimental section.

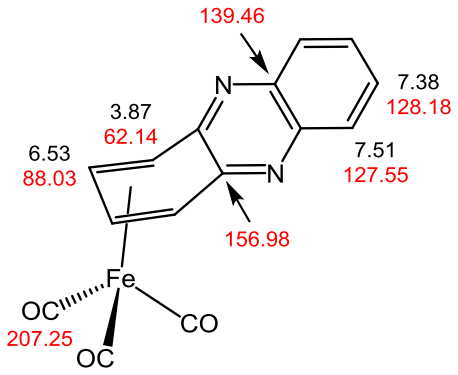

*3.2. Reactions of **1a** and **1b** with monodentate phosphines*

The ligand substitution reactivity of **1a** and **1b** was next explored as a check of the lability of the coordinated heterocycle in the presence of P-donors. Trimethylamine N-oxide initiated reactions of **1a** with $P(OMe)_3$ and PPh_3 at room temperature afforded the mono-substituted products $Fe(CO)_2\{P(OMe)_3\}(\eta^4\text{-}C_{12}H_8N_2)$ (**2a**) and $Fe(CO)_3(PPh_3)(\eta^4\text{-}C_{12}H_8N_2)$ (**3a**) as red crystals in 88 and 95% yields, respectively. The reaction of **1b** with $P(OMe)_3$ and PPh_3 proceeded similarity and furnished $Fe(CO)_2\{P(OMe)_3\}(\eta^4\text{-}C_{13}H_9N)$ (**2b**) (80% yield) and $Fe(CO)_3(PPh_3)(\eta^4\text{-}C_{13}H_9N)$ (**3b**) (88% yield), respectively. Attempts to substitute a second carbonyl in the initial substitution products **2a,b** and **3a,b** by either PPh_3 or $P(OMe)_3$ in the presence of Me_3NO were unsuccessful. In no case was any evidence for the release of the heterocyclic ligand observed.

The data obtained from elemental analyses and IR and NMR spectroscopies corroborate the nature of the products **2a,b** and **3b**, whose structures are depicted in Scheme 4. Further, the solid-state structures of **2a** and **3b** were also established by X-ray crystallography. The ORTEP drawing of molecular structure of **2a** is depicted in Fig. 2, confirming the substitution of a single CO ligand by $P(OMe)_3$ which lies underneath the coordinated phenazine ligand. The figure caption lists selected bond distances and angles for **2a**. The Fe-C(phenazine) bond distances [Fe(1)–C(7) 2.048(4), Fe(1)–C(8) 2.050(4), Fe(1)–C(6) 2.153(4), Fe(1)–C(9) 2.153(4) Å] are comparable in length to those Fe-C bonds in **1a**. The C–C bond lengths in the diene portion of the ligand [C(6)–C(7) 1.428(5), C(7)–C(8) 1.408(4), C(8)–C(9) 1.423(5) Å] are shorter than those carbon-carbon bond lengths associated with the non-coordinated aryl ring [C(6)–C(17) 1.472(5), C(9)–C(10) 1.453(5) Å]. The Fe–P vector exhibits a distance is 2.1647(6) Å, which in turn is intermediate in length compared to the Fe-P bond distance in

[Fe(CO)(COMe)(η^5–MeC_5H_4)(PPh_2Et)] {2.200(2) Å}[46] and [Fe(CO){η^1-C(O)C(Me)=C(Ph)Me}(η^5–C_5H_5)($P(OPh)_3$)] {2.110(1) Å}.[47] The ORTEP drawing of the molecular structure of **3b** is shown in Fig. 3. The molecule is structurally similar to **2a** apart from the terminal PPh_3 ligand and the η^4-acridine ligand. The coordinated PPh_3 adopts one of the two coordination sites at iron that are distal to the heterocycle. The acridine ligand is coordinated to the iron atom in a manner analogous to that of the phenazine ligand in **1a** and **2a**. The Fe–P bond distance is 2.2277(6) Å and is significantly longer than the Fe–P bond distance in **2a**.

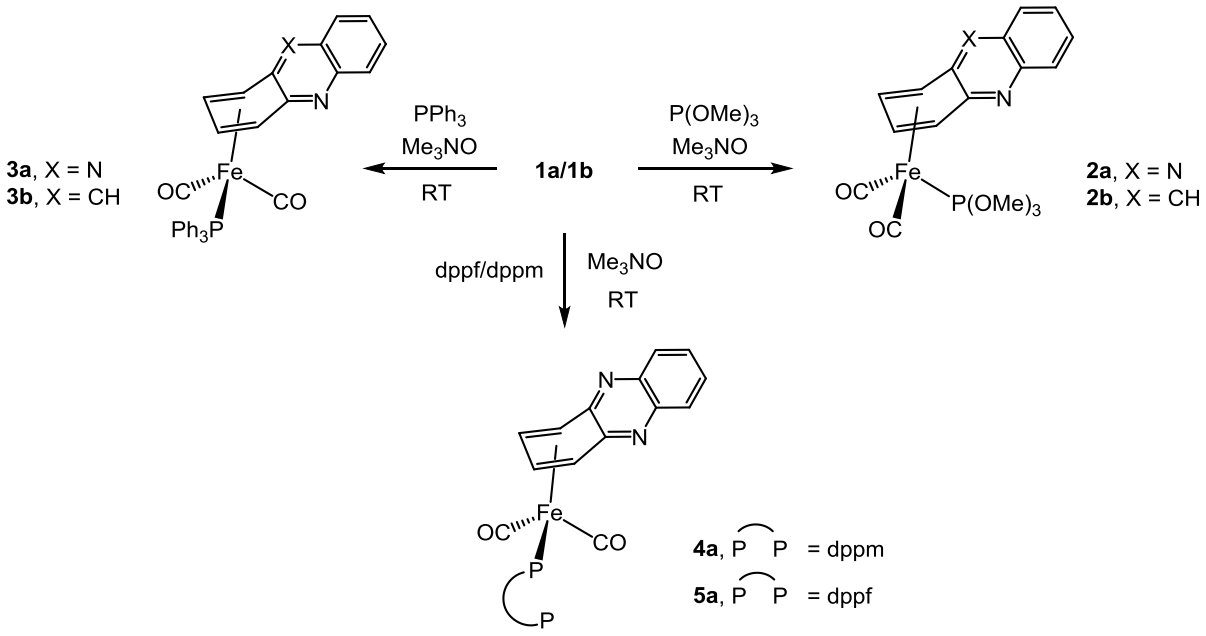

Scheme 4. Reactions of **1a** and **1b** with mono- and bidentate phosphines and phosphite

The IR spectra of compounds **2a,b** and **3a,b** display, as expected, two strong carbonyl stretching frequencies (**2a**: 2008, 1954 cm^{-1}; **2b**: 1999, 1943 cm^{-1}; **3a**: 1997, 1943 cm^{-1}; **3b**: 1988, 1933 cm^{-1}), indicating that the number and arrangement of CO ligands are similar in the four $Fe(CO)_2P(\eta^4$-polyene) species. The shifts of the stretching frequencies to lower wavenumbers going from **1a** and **1b** to **2a,b** and **3a,b** are consistent with increased electron density at the iron center from the replacement of a carbonyl ligand with a P-donor ligand. The ^{31}P NMR spectrum of each compound displays a single resonance at δ 174.6 (**2a**), 177.1 (**2b**), 67.0 (**3a**), and 66.6 **(3b**) for the coordinated phosphite/phosphine ligand. The presence of AA′XX′ and AA′BB′ multiplets in the ^1H NMR spectrum of **2a** are confirmed for the diene and non-coordinated aryl ring protons, and the doublet at δ 3.58 (9H) is readily ascribed

to the methyl protons of the $P(OMe)_3$ ligand. The recorded ^1H NMR data for **2b** are consistent with the proposed structure. Use of PPh_3 as a ligand in the substitution reactions with **1a,b** afforded products similar to those of **2a,b**, and these data are summarized in the experimental section.

*3.3. Reactions of **1a** with diphosphines*

The reactivity of **1a** with the diphosphines dppm and dppf were next examined in order to probe the ligand chelation of these diphosphines at the iron center. Heating **1a** with dppm at 40 ^oC in the presence of Me_3NO afforded the mononuclear complex $Fe(CO)_2(\kappa^1\text{-dppm})(\eta^4\text{-}C_{12}H_8N_2)$ (**4a**) in 40% yield. A comparable product yield was also obtained when the more flexible dppf was employed, furnishing $Fe(CO)_2(\kappa^1\text{-dppf})(\eta^4\text{-}C_{12}H_8N_2)$ (**5a**) in 50 and yield. Compounds **4a** and **5a** have been characterized by a combination of elemental analysis, IR, ^1H and $^{31}P\{^1H\}$ NMR spectroscopies, and by single crystal X-ray diffraction analysis in the case of **4a**. An ORTEP drawing of the molecular structure of **4a** is depicted in Fig. 4 and selected bond distances and angles are reported in the figure caption. The structure of **4a** confirms the replacement of a single CO in **1a** and the presence of a κ^1-coordinated dppm ligand. The Fe-C bond distances to the phenazine ligand [Fe(1)–C(3) 2.121(3), Fe(1)–C(4) 2.032(3), Fe(1)–C(5) 2.040(3), Fe(1)–C(6) 2.131(3) Å] are slightly shorter than those of the corresponding Fe–C bond distances in **1a**. One interesting finding is that among the phenazine carbon atoms coordinated to Fe(1) atom, the two C–C bond lengths are approximately equal [C(3)–C(4) 1.414(5), C(5)–C(6) 1.418(4) Å] and slightly longer than that of the other carbon-carbon bond distance [C(4)–C(5) 1.389(4) Å] define by the diene linkage in **4a**. The Fe–P bond distance is 2.2086(10). The remaining bond distances and angles are unremarkable and require no comment.

The spectroscopic data of **4a** are fully consistent with the solid-state structure. The IR spectra of compounds **4a** and **5a** exhibit a similar pattern of CO stretches, indicating that the number and arrangement of CO ligands are similar in both the species. In addition to the characteristic phenyl and phenazine ring proton resonances in the aromatic region, the aliphatic region of ^1H NMR of **4a** displays diastereotopic protons at δ 3.23 and 3.04 (each integrating to 1H) assigned to the methylene protons of the dppm ligand. In each of **4a** and **5a**, the presence of a dangling diphosphine is easily deduced from the $^{31}P\{^1H\}$ NMR spectra, which exhibit two doublets at δ 57.0 and -24.0 (J = 76.0 Hz) for **4a** and two singlets δ 61.0

and -18.1 for **5a**, consistent with the presence of two nonequivalent phosphorus nuclei. The higher field resonance in each species is confidently assigned to the dangling phosphine moiety.

4. Conclusions

A summary of the reactions described in this report is shown in Schemes 3 and 4. The reaction of phenazine and acridine with $Fe_3(CO)_{12}$ at 80 °C yielded the mononuclear complexes $Fe(CO)_3(\eta^4\text{-}C_{12}H_8N_2)$ (**1a**)[12] and $Fe(CO)_3(\eta^4\text{-}C_{13}H_9N)$ (**1b**) as the sole isolable products. Four new substituted derivatives $Fe(CO)_2P(\eta^4\text{-heterocycle})$ [where P = $P(OMe)_3$ and PPh_3] were prepared from **1a** and **1b** by oxidative decarbonylation of the parent compound upon treatment of Me_3NO in the presence of a P-donor. Similar reactions between **1a** and **1b** and the diphosphines dppm and dppf were also confirmed. The η^4-coordination of a phenazine and acridine ligand to the iron center in our new compounds is unprecedented, and we have structurally established this phenomenon in for compounds **1a**, **2a**, **3b**, and **4a**. The stability of the ancillary phenazine and acridine ligands in arene exchange reactions and site-selective functionalization of the coordinated heterocycle are presently under investigation.

5. Acknowledgements

We thank the Ministry of Science and Information & Communication Technology, Government of the People's Republic of Bangladesh for financial support. MGR thanks the Robert A. Welch Foundation (grant B-1093) for financial support and acknowledges computational resources through UNT's High Performance Computing Services and CASCaM. Prof. Michael B. Hall (TAMU) is thanked for providing us a copy of his *JIMP2* program, which was used to prepare the geometry-optimized structure reported here.

6. Appendix A. Supplementary material

CCDC 1424688, CCDC 1424689, CCDC 1424690 and CCDC 1424705 contain supplementary crystallographic data for **1a**, **2a**, **3b** and **4a** successively. These data may be obtained free of charge from The Cambridge Crystallographic Data Center via www.ccdc.cam.ac.uk/data_request/cif.

Table 1. Crystal data, data collection and structure refinement papameters for compounds **1a**, **2a**, **3b** and **4a.**

Compound	**1a**	**2a**	**3b**	**4a**
Empirical formula	$C_{15}H_8N_2O_3Fe$	$C_{17}H_{17}FeN_2O_5P$	$C_{33}H_{24}FeNO_2P$	$C_{40}H_{32}Cl_2FeN_2O_2P_2$
Formula weight	320.09	416.15	553.35	761.41
Temperature (K)	150(2) K	150(1) K	150(1) K	150(2) K
Wavelength (Å)	Mo Kα, 0.71073	Cu Kα, 1.54184	Cu Kα, 1.54184	MoKα, 0.71073
Crystal system	triclinic	monoclinic	monoclinic	monoclinic
Space group	*P*1 bar	$P2_1$	$P2_1/n$	C2/c
a (Å)	6.7417(14)	6.99641(12)	16.29543(16)	32.239(11)
b (Å)	9.7046(19)	12.87326(19)	8.77976(7)	10.557(4)
c (Å)	10.249(2)	9.95847(17)	18.33151(16)	21.580(7)
α (º)	75.491(3)	90	90	90
β (º)	86.227(3)	99.3910(16)	99.0887(9)	108.522(5)
γ (º)	83.399(3)	90	90	90
Volume ($Å^{-3}$)	644.4(2)	884.90(3)	2589.76(4)	6964(4)
Z	2	2	4	8
Calculated density (g/cm^3)	1.6495	1.5617	1.419	1.4523
Absorption coefficient (mm^{-1})	1.181	7.974	5.505	0.718
F(000)	324.9	427.6	1144.0	3143.9
Crystal size mm^3	0.14 × 0.10 × 0.06	0.3492 × 0.3013 × 0.1082	0.2 × 0.18 × 0.04	0.65 × 0.40 × 0.18
2θ range for data collection (º)	7.22 to 56.4	12.82 to 147.92	6.748 to 147.248	5.34 to 57.16
Limiting indices	$-8 \le h \ge 8$ $-12 \le k \ge 12$ $-13 \le l \ge 13$	$-8 \le h \ge 8$ $-11 \le k \ge 16$ $-12 \le l \ge 11$	$-20 \le h \le 19$ $-10 \le k \le 10$ $-22 \le l \le 22$	$-42 \le h \ge 42$ $-13 \le k \ge 13$ $-28 \le l \ge 28$
Reflections collected	5344	5128	45422	28372
Independent reflections(R_{int})	2776 [0.0332]	2597 [0.0342]	5182 [0.0360]	8201 [0.0648]
Refinement method	Full-matrix least-squares on F^2	Full-matrix least-squares on F^2	Full-matrix least-squares on F^2	Full-matrix least-squares on F^2
Data / restraints / parameters	2776/0/221	2597/0/237	5182/0/343	8201/0/444
Goodness-of-fit on F^2	1.049	1.053	1.133	0.912
Final R indices [$I > 2\sigma(I)$]	R_1 = 0.0327, wR_2 = 0.0819	R_1 = 0.0369, wR_2 = 0.0945	R_1 = 0.0348 wR_2 = 0.0816	R_1 = 0.0551, wR_2 = 0.1263
R indices (all data)	R_1 = 0.0365, wR_2= 0.0845	R_1 = 0.0378, wR_2 = 0.0957	R_1 = 0.0364 wR_2 = 0.0824	R_1 = 0.0989, wR_2 = 0.1463
Largest diff. peak/hole ($e.Å^{-3}$)	0.63 and –0.42	1.21 and –0.62	0.41 and –0.33	1.20 and –0.55

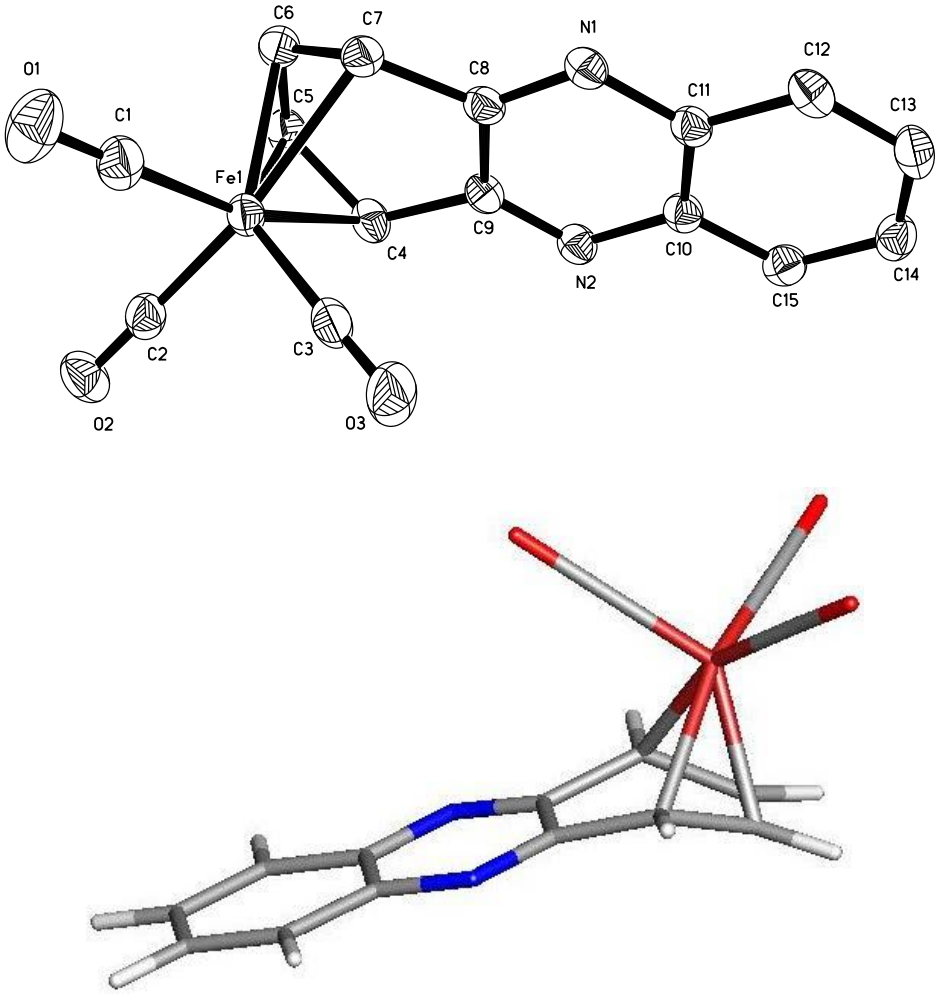

Fig. 1. ORTEP drawing of the molecular structure of $Fe(CO)_3(\eta^4\text{-}C_{12}H_8N_2)$ (**1a**; top), showing 50% probability thermal ellipsoids (hydrogen atoms are omitted for clarity) and DFT-optimized structure of **A** (bottom). Selected X-ray diffraction bond lengths (Å) and angles (°): Fe(1)–C(1) 1.798(2), Fe(1)–C(2) 1.7961(19), Fe(1)–C(3) 1.8070(19), Fe(1)–C(4) 2.1517(19), Fe(1)–C(5) 2.0585(18), Fe(1)–C(6) 2.0566(18), Fe(1)–C(7) 2.1567(18), C(4)–C(5) 1.428(3), C(4)–C(9) 1.470(2), C(5)–C(6) 1.399(3), C(6)–C(7) 1.430(3), C(7)–C(8) 1.466(2), C(8)–C(9) 1.437(2), N(1)–C(8) 1.309(2), N(1)–C(11) 1.382(2), N(2)–C(9) 1.307(2), N(2)–C(10) 1.393(2), C(10)–C(11) 1.410(3), C(11)–C(12) 1.411(2), C(12)–C(13) 1.373(3), C(13)–C(14) 1.401(3), C(14)–C(15) 1.375(3), C(10)–C(15) 1.408(3), C(1)–Fe(1)–C(2) 91.46(9), C(2)–Fe(1)–C(3) 100.60(8), C(1)–Fe(1)–C(3) 99.54(9), C(1)–Fe(1)–C(4) 163.33(8), C(2)–Fe(1)–C(4) 93.89(8), C(3)–Fe(1)–C(4) 94.98(8), C(1)–Fe(1)–C(5) 124.39(8), C(2)–Fe(1)–C(5) 93.26(8), C(3)–Fe(1)–C(5) 133.54(8), C(4)–Fe(1)–C(5) 39.56(7), C(1)–Fe(1)–C(6) 94.25(8), C(2)–Fe(1)–C(6) 122.66(8), C(3)–Fe(1)–C(6) 134.13(8), C(5)–Fe(1)–C(6) 39.74(8), C(4)–Fe(1)–C(5) 69.60(7), C(1)–Fe(1)–C(7) 93.62(8), C(2)–Fe(1)–C(7) 161.85(8), C(3)–Fe(1)–C(7) 95.72(8), C(6)–Fe(1)–C(7) 39.58(7), C(5)–Fe(1)–C(7) 69.55(7), C(4)–Fe(1)–C(7) 76.72(7).

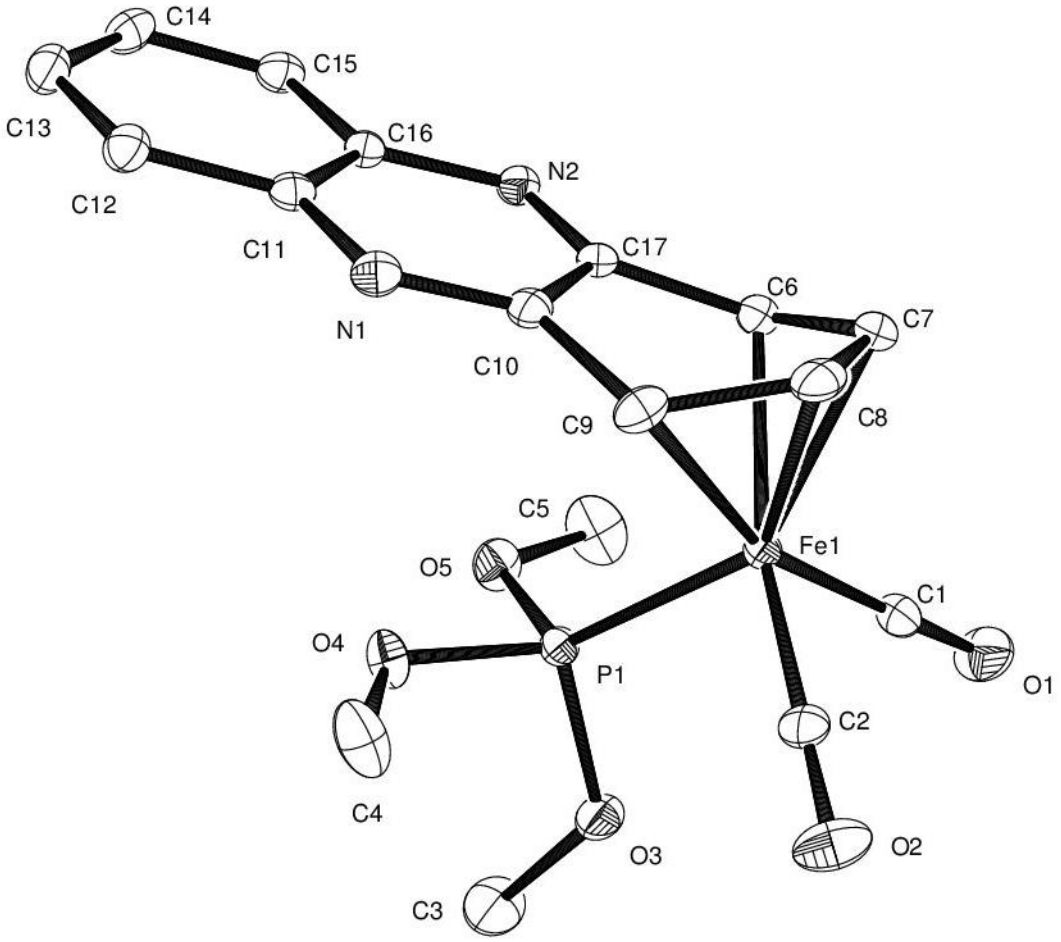

Fig. 2. ORTEP drawing of the molecular structure of $Fe(CO)_2\{P(OMe)_3\}(\eta^4\text{-}C_{12}H_8N_2)$ (**2a**), showing 50% probability thermal ellipsoids. Hydrogen atoms are omitted for clarity. Selected bond lengths (Å) and angles (º): Fe(1)–C(1) 1.773(4), Fe(1)–C(2) 1.772(4), Fe(1)–C(6) 2.153(4), Fe(1)–C(7) 2.048(4), Fe(1)–C(8) 2.050(4), Fe(1)–C(9) 2.153(4), Fe(1)–P(1) 2.1647(6), C(6)–C(7) 1.428(5), C(6)–C(17) 1.472(5), C(7)–C(8) 1.408(4), C(8)–C(9) 1.423(5), C(9)–C(10) 1.453(5), C(10)–C(17) 1.454(3), N(1)–C(10) 1.308(5), N(1)–C(11) 1.371(4), N(2)–C(16) 1.394(4), N(2)–C(17) 1.305(5), C(11)–C(12) 1.411(5), C(11)–C(16) 1.420(3), C(12)–C(13) 1.369(5), C(13)–C(14) 1.405(4), C(14)–C(15) 1.376(5), C(15)–C(16) 1.396(5), C(1)–Fe(1)–C(2) 90.99(11), C(1)–Fe(1)–P(1) 95.94(13), C(2)–Fe(1)–P(1) 96.18(13), C(1)–Fe(1)–C(6) 93.31(17), C(2)–Fe(1)–C(6) 162.51(17), P(1)–Fe(1)–C(6) 100.21(11), C(1)–Fe(1)–C(7) 93.31(17), C(2)–Fe(1)–C(7) 123.19(17), P(1)–Fe(1)–C(7) 139.32(11), C(6)–Fe(1)–C(7) 39.64(15), C(1)–Fe(1)–C(8) 123.84(17), C(2)–Fe(1)–C(8) 93.76(17), P(1)–Fe(1)–C(8) 138.75(11), C(7)–Fe(1)–C(8) 40.19(11), C(6)–Fe(1)–C(8) 69.83(16), C(1)–Fe(1)–C(9) 162.80(18), C(2)–Fe(1)–C(9) 94.22(16), P(1)–Fe(1)–C(9) 99.77(11), C(8)–Fe(1)–C(9) 39.49(15), C(7)–Fe(1)–C(9) 70.09(16), C(6)–Fe(1)–C(9) 77.10(10).

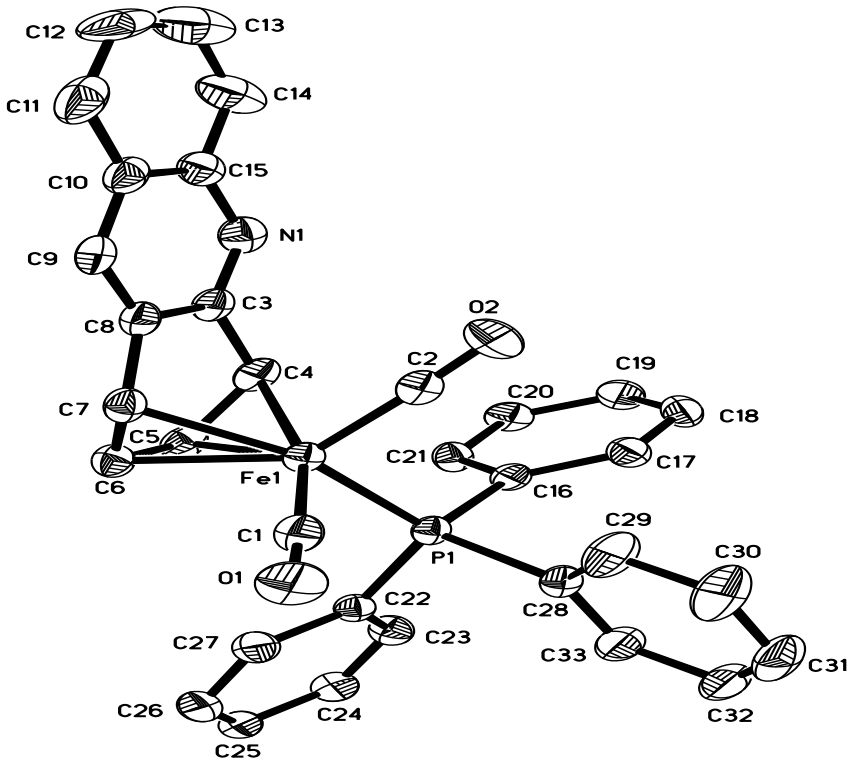

Fig. 3. ORTEP drawing of the molecular structure of $Fe(CO)_2(PPh_3)(\eta^4\text{-}C_{13}H_9N)$ (**3b**), showing 50% probability thermal ellipsoids. Hydrogen atoms are omitted for clarity. Selected bond lengths (Å) and angles (°): Fe(1)–P(1) 2.2277(6), Fe(1)–C(4) 2.1585(19), Fe(1)–C(5) 2.054(2), Fe(1)–C(6) 2.051(2), Fe(1)–C(7) 2.143(2), N(1)–C(3) 1.321(3), N(1)–C(15) 1.399(3), C(3)–C(4) 1.469(3), C(4)–C(5) 1.422(3), C(5)–C(6) 1.406(3), C(6)–C(7) 1.432(3), C(7)–C(8) 1.466(3), C(3)–C(8) 1.434(3), C(4)–Fe(1)–P(1) 97.90(6), C(5)–Fe(1)–P(1) 92.74(6), C(5)–Fe(1)–C(4) 39.35(8), C(5)–Fe(1)–C(7) 69.78(8), C(6)–Fe(1)–P(1) 119.05(7), C(6)–Fe(1)–C(4) 69.60(8), C(6)–Fe(1)–C(5) 40.07(9), C(6)–Fe(1)–C(7) 39.86(9), C(7)–Fe(1)–P(1) 158.90(6), C(7)–Fe(1)–C(4) 76.33(8), C(6)–C(7)–Fe(1) 66.59(11), C(6)–C(7)–C(8)119.87(18), C(8)–C(7)–Fe(1) 104.24(13), C(3)–C(8)–C(7) 114.45(18), C(9)–C(8)–C(3) 120.0(2), C(9)–C(8)–C(7) 125.44(19), C(8)–C(9)–C(10) 118.6(2), N(1)–C(3)–C(4) 121.45(18), N(1)–C(3)–C(8) 123.56(19), C(8)–C(3)–C(4) 114.88(18), C(3)–C(4)–Fe(1) 103.35(12), C(5)–C(4)–Fe(1) 66.35(11), C(5)–C(4)–C(3) 119.80(19), C(4)–C(5)–Fe(1) 74.31(11), C(6)–C(5)–Fe(1) 69.85(12), C(6)–C(5)–C(4) 116.45(19), C(5)–C(6)–Fe(1) 70.08(12), C(5)–C(6)–C(7) 115.60(19), C(7)–C(6)–Fe(1) 73.56(12).

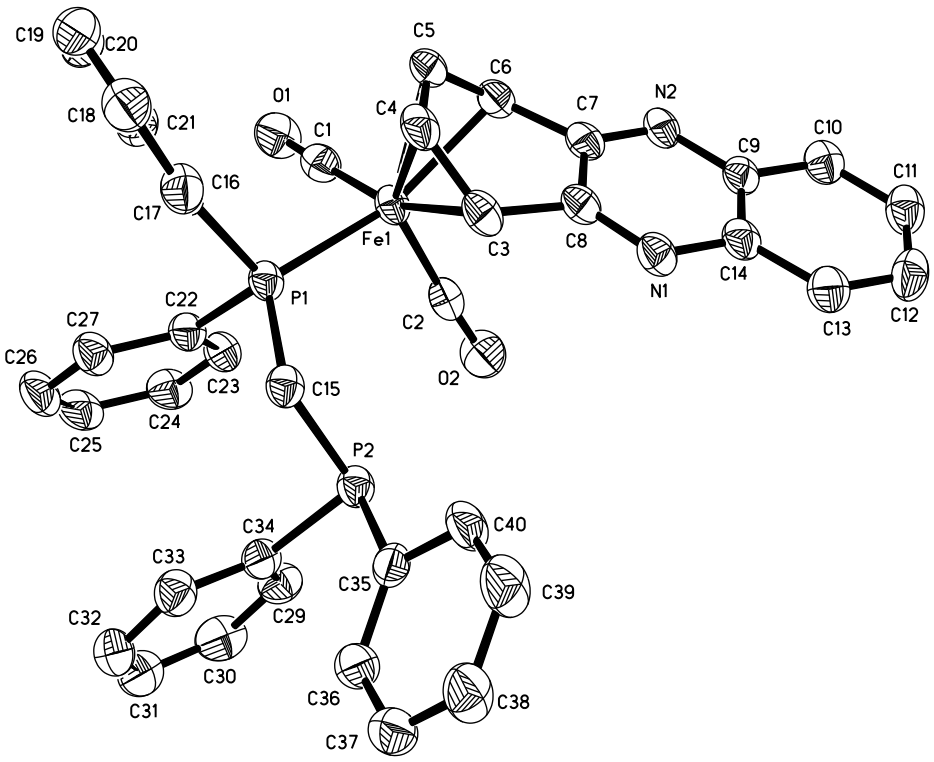

Fig. 4. ORTEP drawing of the molecular structure of $Fe(CO)_2(dppm)(\eta^4\text{-}C_{12}H_8N_2)$ (**4a**), showing 50% probability thermal ellipsoids. Hydrogen atoms are omitted for clarity. Selected bond lengths (Å) and angles (°): Fe(1)–C(1) 1.757(3), Fe(1)–C(2) 1.771(4), Fe(1)–C(3) 2.121(3), Fe(1)–C(4) 2.032(3), Fe(1)–C(5) 2.040(3), Fe(1)–C(6) 2.131(3), Fe(1)–P(1) 2.2086(10), C(3)–C(4) 1.414(5), C(3)–C(8) 1.451(4), C(4)–C(5) 1.389(4), C(5)–C(6) 1.418(4), C(6)–C(7) 1.450(4), C(7)–C(8) 1.439(4), N(2)–C(7) 1.2297(4), N(1)–C(8) 1.298(4), N(1)–C(14) 1.381(4), N(2)–C(9) 1.376(4), C(9)–C(14) 1.399(4), C(9)–C(10) 1.405(4), C(10)–C(11) 1.360(5), C(11)–C(12) 1.391(5), C(12)–C(13) 1.371(5), C(13)–C(14) 1.390(4), C(1)–Fe(1)–C(2) 100.55(15), C(1)–Fe(1)–P(1) 89.36(11), C(2)–Fe(1)–P(1) 100.19(10), C(1)–Fe(1)–C(4) 122.99(14), C(2)–Fe(1)–C(4) 134.79(14), C(1)–Fe(1)–C(5) 92.68(14), C(2)–Fe(1)–C(5) 137.58(14), C(4)–Fe(1)–C(5) 39.89(13), C(1)–Fe(1)–C(3) 162.15(14), C(2)–Fe(1)–C(3) 95.61(14), C(4)–Fe(1)–C(3) 39.73(12), C(5)–Fe(1)–C(3) 70.11(13), C(1)–Fe(1)–C(6) 92.93(13), C(2)–Fe(1)–C(6) 99.06(13), C(4)–Fe(1)–C(6) 69.56(13), C(5)–Fe(1)–C(6) 39.68(12), C(3)–Fe(1)–C(6) 76.99(12), C(3)–Fe(1)–P(1) 95.21(9), C(4)–Fe(1)–P(1) 92.47(10), C(5)–Fe(1)–P(1) 120.24(10), C(6)–Fe(1)–P(1) 159.84(9).

References

[1] R.M. Hochstrasser, J. Chem. Phys. 36 (1962) 1808.

[2] A.J. Kallir, G.W. Suter, U.P. Wild, J. Phys. Chem. 89 (1985) 1996.

[3] J.J. Aaron, M. Maafi, C.Parkanyi, C. Boniface, Spectrochim. Acta 51A (1995) 603.

[4] Y. Hirata, I. Tanaka, Chem. Phys. Lett. 43 (1976) 568.

[5] A. Grabowska, Chem. Phys. Lett.1 (1967) 1113.

[6] T.G. Pavlopoulos, Spectrochim. Acta 43A (1987)715.

[7] J.I. Del Barrio, J.R. Rebato, F.M.G.- Tablas, J. Phys. Chem., 1989, **93**, 6836.

[8] V.A. Kuzmin, P.P. Levin, Bull. Acad. Sci. USSR Div. Chem. Sci. 1988, **37**, 1098.

[9] (a) W. Maniukiewicz, M. Bukowska-Strzyzewska, M. Sadowska, Acta Cryst. E 60 (2004) m73. (b) R.T. Schneider, C.P. Landee, M.M. Turnbull, F.F. Awwadi, B. Twamley, Polyhedron 26 (2007) 1849.

[10] (a) F.A.Cotton, T.R. Felthouse, Inorg. Chem. 20 (1981) 600. (b) F.A. Cotton, Y.Kim,T.Ren, Inorg. Chem. 31 (1992) 2723. (c) J. Scholz, A. Scholz, R. Weimann, C. Janiak, H. Schumann, Angew. Chem., Int. Ed. 33 (1994) 1171. (d) M. Munakata, T. Kuroda-Sowa, M. Maekawa, A. Honda, S. Kitagawa, J. Chem. Soc., Dalton Trans. (1994) 2771. (e) T. Kuroda-Sowa, M. Munakata, H. Matsuda, S. Akiyama, M.J. Maekawa, J. Chem. Soc., Dalton Trans. (1995) 2201. (f) J.A. Whiteford, P.J. Stang, S.D. Huang, Inorg. Chem. 37 (1998)5595. (g) S.R. Batten, B.F. Hoskins, R. Robson, New J. Chem. 22 (1998) 173. (h) D.J. Chesnut, D. Plewak, J. Zubieta, J. Chem. Soc., Dalton Trans. (2001) 2567. (i) H. Miyasaka, R. Clerac, C.S. Campos-Fernández, K.R. Dunbar, J. Chem. Soc., Dalton Trans. (2001) 858. (j) Z. Shi, X. Gu, J. Peng, Z. Xin, Eur. J. Inorg. Chem. (2005) 3811. (k) T. Kogane, N.Koyama, T. Ishida, T. Nogami, Polyhedron 26 (2007), 1811. (l) J.Q. *Sha*, *J. Peng*, A.X. *Tian*, H.S. *Liu*, *J. Chen*, *Cryst. GrowthDes. 7* (*2007*). *2535.* (m) T. Schneider, C.P. Landee, M.M. Turnbull, F.F. Awwadi, B. Twamley, Polyhedron 26 (2007) 1849. (n) J. Q. Sha, J. Peng, Y. Li, P. P. Zhang, H. J. Pang, Inorg. Chem. Commun. 11 (2008) 907. (o) S.E.H. Etaiw, D.M.A. El-Aziz, M.S. Ibrahim, A.S.B.El-din, Polyhedron 28 (2009) 1001. (p) W.J. Evans, S.E. Lorenz, J.W. Ziller, Inorg. Chem. 48 (2009) 2001.

[11] M. Munakata, S. Kitagawa, N. Ujimaru, M. Nakamura, M. Maekawa, H.Matsuda, Inorg. Chem. 32 (1993) 826.

[12] R.A. Bauer, E.O. Fischer, C.G. Kreiter, J. Organomet. Chem. 24 (1970) 737.

[13] W.W. Brennessel, R.E. Jilek, J.E. Ellis, Angew. Chem., Int. Ed. Engl. 46 (2007) 6132.

[14] M.I. Bruce, M.G. Humphrey, M. R. Snow, E.R.T. Tiekink, R.C. Wallis, J. Organomet. Chem. 314 (1986) 311.

[15] N.E. Leadbeater, J. Lewis, P.R. Raithby, G.N. Ward, J. Chem. Soc., Dalton Trans. (1997) 2511.

[16] D. Ellis, L.F. Farrugia, J. Cluster. Sci, 7 (1996) 71.

[17] A. Eisenstadt, C.M. Giandomenico, M.F. Frederick, R.M. Laine, *Organometallics*, 1985, **4**, 2033.

[18] G.A. Foulds, B.F.G. Johnson, J. Lewis, J. Organomet. Chem. 294 (1985) 123.

[19] J.A. Cabeza, I. del Río, E. Pérez-Carreño, V. Pruneda, Organometallics, 30 (2011) 1148.

[20] J.A. Cabeza, I. del Río, M.C. Goite, E. Pérez-Carreño, V. Pruneda, Chem. Eur. J. 15 (2009) 7339.

[21] A. Eisenstadt, C.M. Giandomenico, M.F. Frederick, R.M. Laine, Organometallics 4 (1985) 2033.

[22] C.C. Yin, A.J. Deeming, J. Chem. Soc., Dalton Trans. (1975) 2091.

[23] R.H. Fish, T.J. Kim, J.L. Steward, J.H. Bushweller, R.K. Rosen, J. W. Dupon. Organometallics, 5 (1986) 2193.

[24] J.A. Cabeza, P. Garcia-Alvarez, V. Pruneda, Organometallics, 31 (2012) 941.

[25] Md. A. H. Chowdhury, S. Rajbangshi , A. Rahaman , L. Yang, V. N. Nesterov, M. G. Richmond, S. M. Mobin, S. E. Kabir, J. Organomet. Chem. 779 (2015) 21.

[26] W. McFarlane, G. Wilkinson, Inorg. Synth. 8 (1966) 181.

[27] SMART Version 5.628; Bruker AXS, Inc., 5465 East Cheryl Parkway, Madison, WI 53711-5373, 2003.

[28] SMART Version 5.628; Bruker AXS, Inc., 5465 East Cheryl Parkway, Madison, WI 53711-5373, 2003.

[29] G.M. Sheldrick, SADABS Version 2.10; University of Göttingen, Göttingen, Germany, 2003.

[30] O.V. Dolomanov, L.J. Bourhis, R.J. Gildea, J.A.K. Howard, H. Puschmann, J. Appl. Cryst. 42 (2009) 339-341.

[31] G.M. Sheldrick, Acta Cryst. A64 (2008) 112-122.

[32] L.J. Bourhis, O.V. Dolomanov, R.J. Gildea, J.A.K. Howard, H. Puschmann, 2013, in preparation.

[33] M. J. Frisch, G. W. Trucks, H. B. Schlegel, G. E. Scuseria, M. A. Robb, J. R. Cheeseman, G. Scalmani, V. Barone, B. Mennucci, G. A. Petersson, H. Nakatsuji, M. Caricato, X. Li, H. P. Hratchian, A. F. Izmaylov, J. Bloino, G. Zheng, J. L. Sonnenberg, M. Hada, M. Ehara, K. Toyota, R. Fukuda, J. Hasegawa, M. Ishida, T. Nakajima, Y. Honda, O. Kitao, H. Nakai, T. Vreven, J. A. Montgomery, Jr., J. E. Peralta, F. Ogliaro, M. Bearpark, J. J. Heyd, E. Brothers, K. N. Kudin, V. N. Staroverov, R. Kobayashi, J. Normand, K. Raghavachari, A. Rendell, J. C. Burant, S. S. Iyengar, J. Tomasi, M. Cossi, N. Rega, J. M. Millam, M. Klene, J. E. Knox, J. B. Cross, V. Bakken, C. Adamo, J. Jaramillo, R. Gomperts, R. E. Stratmann, O. Yazyev, A. J. Austin, R. Cammi, C. Pomelli, J. W. Ochterski, R. L. Martin, K. Morokuma, V. G. Zakrzewski, G. A. Voth, P. Salvador, J. J. Dannenberg, S. Dapprich, A. D. Daniels, O. Farkas, J. B. Foresman, J. V. Ortiz, J. Cioslowski, D. J. Fox, Gaussian 09, Revision A.02, Gaussian, Inc., Wallingford CT, 2009.

[34] A. D. Becke, J. Chem. Phys. 98 (1993) 5648.

[35] C. Lee, W. Yang, R. G. Parr, Phys. Rev. B 37 (1988), 785.

[36] (a) M. Dolg, U. Wedig, H. Stoll, H. Preuss, J. Chem. Phys. 86 (1987) 866. (b) S. P. Walch, C. W. Bauschlicher, J. Chem. Phys. 78 (1983) 4597.

[37] (a) G. A. Petersson, A. Bennett, T. G. Tensfeldt, M. A. Al-Laham, W. A. Shirley, J. Mantzaris, J. Chem. Phys. 89 (1988) 2193. (b) G. A. Petersson, M. A. Al-Laham, J. Chem. Phys. 94 (1991) 6081.

[38] A.E. Reed, L.A. Curtiss, F. Weinhold, Chem. Rev. 88 (1988) 899.

[39] K.B. Wiberg, Tetrahedron 24 (1968) 1083.

[40] (a) JIMP2, version 0.091, a free program for the visualization and manipulation of molecules: M. B. Hall, R. F. Fenske, Inorg. Chem. 11 (1972) 768. (b) J. Manson, C. E. Webster, M. B. Hall, Texas A&M University, College Station, TX, 2006: http://www.chem.tamu.edu/jimp2/index.html.

[41] A. Sattler, G. Zhu, G. Parkin, J. Am. Chem. Soc. 131 (2009) 7828.

[42] Q. Dong, J.-H. Su, S. Gong, Q.-S. Li, Y. Zhao, B. Wu, X.-J. Yang, Organometallics 32 (2013) 2866.

[43] (a) G.J. Reiss, Acta Crystallogr. Sect. E Struct. Rep. Online 66 (2010) m1369 and references therein. (b) S.L. Ingham, S.W. Magennis, J. Organomet. Chem. 574 (1999) 302. (c) K.S. Claire, O.W. Howarth, A. McCamley, J. Chem. Soc., Dalton Trans. (1994) 2615. (d) R. Goddard, P. Woodward, , J. Chem. Soc., Dalton Trans. (1979) 661. (e) T. Ando, N. Nakata, K. Suzuki, T. Matsumoto, , J. Chem. Soc., Dalton Trans. 41 (2012) 1678.

[44] (a) T.A. Albright, P. Hofmann, R. Hoffmann, J. Am. Chem. Soc. 99 (1977) 7546. (b) M. Bühl, W. Thiel, Inorg. Chem. 36 (1997) 2922.

[45] L. Kruczynski, J. Takats, Inorg. Chem. 15 (1976) 3140.

[46] H.Ye. Liu, Md.M. Rahman, L.L. Koh, K. Eriks, W.P. Giering, A. Prock, Acta. Cryst. C45 (1989) 1683.

[47] D.L. Reger, E. Mintz, L. Lebioda, J. Am. Chem. Soc. 108 (1986) 1940.